CCR5 inhibition in critical COVID-19 patients decreases inflammatory cytokines, increases CD8 T-cells, and decreases SARS-CoV2 RNA in plasma by day 14

Bruce K. Patterson[a,*], Harish Seethamraju[b], Kush Dhody[c], Michael J. Corley[d], Kazem Kazempour[c], Jay Lalezari[e], Alina P.S. Pang[d], Christopher Sugai[f], Eisa Mahyari[g], Edgar B. Francisco[a], Amruta Pise[a], Hallison Rodrigues[a], Helen L. Wu[g], Gabriela M. Webb[g], Byung S. Park[g], Scott Kelly[h], Nader Pourhassan[h], Alina Lelic[i], Lama Kdouh[i], Monica Herrera[j], Eric Hall[j], Benjamin N. Bimber[g], Matthew Plassmeyer[k], Raavi Gupta[l], Oral Alpan[k], Jane A. O'Halloran[m], Philip A. Mudd[n], Enver Akalin[b], Lishomwa C. Ndhlovu[d,1], Jonah B. Sacha[g,1]

[a] IncellDX, Menlo Park, CA, USA
[b] Montefiore Medical Center, New York, NY, USA
[c] Amarex Clinical Research LLC, Germantown, MD, USA
[d] Division of Infectious Diseases, Department of Medicine, Weill Cornell Medicine, New York, NY, USA
[e] Quest Clinical Research, San Francisco, CA, USA
[f] University of Hawaii, Honolulu, HI, USA
[g] Vaccine & Gene Therapy Institute and Oregon National Primate Research Center, Oregon Health & Science University, Portland, OR, USA
[h] CytoDyn Inc., Vancouver, WA, USA
[i] Beckman Coulter, Miami, FL, USA
[j] Bio-Rad, Pleasanton, CA, USA
[k] Amerimmune LLC, Fairfax, VA, USA
[l] State University of New York-University Hospital of Brooklyn, NY, USA
[m] Division of Infectious Diseases, Department of Internal Medicine, USA
[n] Department of Emergency Medicine, Washington University in Saint Louis School of Medicine, Saint Louis, MO, USA

ABSTRACT

Objective: Infection with severe acute respiratory syndrome coronavirus 2 (SARS-CoV-2) is now a global pandemic. Emerging results indicate a dysregulated immune response. Given the role of CCR5 in immune cell migration and inflammation, we investigated the impact of CCR5 blockade via the CCR5-specific antibody leronlimab on clinical, immunological, and virological parameters in severe COVID-19 patients.
Methods: In March 2020, 10 terminally ill, critical COVID-19 patients received two doses of leronlimab via individual emergency use indication. We analyzed changes in clinical presentation, immune cell populations, inflammation, as well as SARS-CoV-2 plasma viremia before and 14 days after treatment.
Results: Over the 14-day study period, six patients survived, two were extubated, and one discharged. We observed complete CCR5 receptor occupancy in all donors by day 7. Compared with the baseline, we observed a concomitant statistically significant reduction in plasma IL-6, restoration of the CD4/CD8 ratio, and resolution of SARS-CoV2 plasma viremia (pVL). Furthermore, the increase in the CD8 percentage was inversely correlated with the reduction in pVL (r = −0.77, p = 0.0013).
Conclusions: Our study design precludes clinical efficacy inferences but the results implicate CCR5 as a therapeutic target for COVID-19 and they form the basis for ongoing randomized clinical trials.

Introduction

* Corresponding author at: IncellDx, Inc, 1541 Industrial Road, San Carlos, CA 94070, USA.
    E-mail address: brucep@incelldx.com (B.K. Patterson).
  [1] Co-senior authors.

Since the initial cases of coronavirus disease 2019 (COVID-19) were reported from Wuhan, China in December 2019 (Huang et al., 2020),

severe acute respiratory syndrome coronavirus 2 (SARS-CoV-2) has emerged as a global pandemic and increasing numbers of severe and critical cases have required invasive external ventilation, which threatens to overwhelm health care systems (World Health Organization, 2020). It remains unclear why COVID-19 patients experience a spectrum of clinical outcomes ranging from asymptomatic to severe disease, where the features of critical COVID-19 include rampant inflammation and cytokine release syndrome (CRS) leading to acute respiratory distress syndrome (ARDS) (Mehta et al., 2020; Qin et al., 2020). Indeed, excessive immune cell infiltration into the lung, CRS, and ARDS have previously been described as defining features of severe disease in humans infected with the closely related betacoronaviruses SARS-CoV and MERS-CoV (Channappanavar and Perlman, 2017; Nicholls et al., 2003). SARS-CoV-infected airway epithelial cells and macrophages express high levels of CCL5 (Law et al., 2005; Yen et al., 2006), which is a chemotactic molecule that can amplify inflammatory responses toward immunopathology, so we hypothesized that disrupting the CCL5–CCR5 axis via the leronlimab-mediated CCR5 blockade might prevent pulmonary trafficking of pro-inflammatory leukocytes and dampen pathogenic immune activation in COVID-19.

Leronlimab, formerly known as PRO 140, is a CCR5-specific human IgG4 monoclonal antibody in development for HIV therapy as a once weekly, at home subcutaneous injection. In five completed and four ongoing HIV clinical trials where over 800 individuals received leronlimab, no drug-related deaths, serious injection site reactions, or drug–drug interactions were reported (Jacobson et al., 2008, 2010a; Jacobson et al., 2010b; Dhody et al., 2018). Subcutaneous, self-administration of leronlimab by patients facilitates simple, once weekly dosing. In contrast to the small molecule CCR5 inhibitors that prevent HIV Env binding to CCR5 via allosteric modulation, leronlimab binds to the CCR5 extracellular loop 2 domain and N-terminus, thereby directly blocking the binding of HIV Env to the CCR5 co-receptor via a competitive mechanism. Leronlimab does not downregulate CCR5 surface expression or deplete CCR5-expressing cells, but it does prevent CCL5-induced calcium mobilization in CCR5+ cells with an IC_{50} of 45 μg/mL (Olson et al., 1999). This ability to specifically prevent CCL5-induced activation and chemotaxis of inflammatory CCR5+ macrophages and T cells suggests that leronlimab might be effective in mitigating pathologies involving the CCR5-ligand pathway.

Methods

Patients

All leronlimab-treated patients were enrolled in this study under an individual patient emergency use investigation new drug (EIND) via a United States Food and Drug Administration (FDA) emergency use authorization. The Albert Einstein College of Medicine Institution Review Board reviewed and approved this study. One 8 mL ethylenediaminetetraacetic acid (EDTA) tube and one 4 mL plasma preparation tube were drawn by venipuncture at day 0 (pre-treatment) and day 3, day 7, and day 14 post-treatment. Peripheral blood mononuclear cells (PBMCs) were isolated from peripheral blood using a Lymphoprep density gradient (STEMCELL Technologies, Vancouver, Canada). Aliquots of cells were frozen in media that contained 90% fetal bovine serum (Hyclone, Logan, UT, USA) and 10% dimethyl sulfoxide (Sigma–Aldrich, St. Louis, MO, USA), and stored at −70 °C. The five COVID observational control patients were part of a prospective observational cohort of subjects with viral respiratory illness symptoms who presented to Barnes Jewish Hospital, St. Louis Children's Hospital, or affiliated Barnes Jewish Hospital testing sites located in Saint Louis, MO, USA. Inclusion criteria required that subjects were symptomatic and had a physician-ordered SARS-CoV-2 test performed in the course

of their normal clinical care. All samples were collected at the time of enrollment, which was during or immediately following evaluation in a medical facility. The study was reviewed and approved by the Washington University Saint Louis Institutional Review Board (WU-350 study approval # 202003085). The study complied with the ethical standards of the Helsinki Declaration.

Assessment of plasma cytokine and chemokine levels

Fresh plasma was employed for cytokine quantification using a customized 13-plex bead-based flow cytometric assay (Legend-Plex, Biolegend, Inc., San Diego, CA, USA) conducted with a CytoFlex flow cytometer. Raw data were analyzed using Legend-Plex software (Biolegend Inc., San Diego, CA, USA). Samples were run in duplicate. In addition, split sample confirmation testing was performed by enzyme-linked immunosorbent assay (MDBiosciences, Minneapolis, MN, USA). Samples falling outside the linear range of the appropriate standard curves were diluted and repeated, where the dilution factor was incorporated into the final average. The cytokines, chemokines, and growth factors analyzed comprised: sCD40L, EGF, eotaxin, fibroblast growth factor (FGF)-2, fms-like tyrosine kinase 3 (Flt-3), fractalkine, granulocyte colony-stimulating factor (G-CSF), granulocyte-macrophage colony-stimulating factor (GM-CSF), growth-regulated oncogene (GRO)-α, FNα2, interferon (IFN)γ, interleukin (IL)-1α, IL-1β, IL-1ra, IL-2, IL-3, Il-4, IL-5, IL-5, IL-6, IL-7, IL-8, IL-9, IL-10, IL-2 (p40), IL-12 (p70), IL-13, IL-15, IL-17A, IL-17E/IL-25, IL-17F, IL-18, IL-22, IL-27, interferon gamma-induced protein 10 (IP-10), monocyte chemoattractant protein (MCP)-1, monocyte-chemotactic protein (MCP)-3, macrophage colony-stimulating factor (M-CSF), macrophage-derived chemokine (MDC), monokine induced by IFN-γ (MIG), macrophage inflammatory protein (MIP)-1α, MIP-1β, platelet-derived growth factor (PDGF)-AA, PDGF-AB/BB, RANTES (regulated on activation, normal T cell expressed and secreted), transforming growth factor (TGF)-α, tumor necrosis factor (TNF)-α, TNF-β, and vascular endothelial growth factor (VEGF).

Flow cytometry

PBMCs were isolated from peripheral blood using a Lympho-prep density gradient (STEMCELL Technologies, Vancouver, Canada). Each sample received a cocktail containing 10 μL Brilliant Stain Buffer (BD Biosciences, Franklin Lakes, NJ, USA), 5 μL True-Stain Monocyte Blocker (BioLegend, San Diego, CA, USA), and the following surface marker antibodies: anti-CD19 (PE-Dazzle594), anti-CD3 (APC), anti-CD16 (Alexa700), HLA-DR (APC/Fire750), and anti-CTLA-4 (PE-Cy7). The following antibodies were then added to each tube individually: anti-CD8 (BUV496), anti-CD4 (BUV661), anti-CD45 (BUV805), anti-CD103 (BV421), anti-TIM3 (BV605), anti-CD56 (BV650), anti-LAG-3 (BV711), anti-CD14 (BB785), and anti-PD-1 (BB700), before incubating at room temperature for 30 min. Cells were fixed and permeabilized in 1× incellMAX (IncellDx, San Carlos, CA, USA) for 60 min at room temperature in the dark. Cells were washed once with 2% bovine serum albumin (BSA) solution, and analyzed using a Cytoflex LX system with 355 nm (20 mW), 405 nm (80 mW), 488 nm (50 mW), 561 nm (30 mW), 638 nm (50 mW), and 808 nm (60 mW) lasers (Beckman Coulter Life Sciences, Indianapolis, IN, USA). Analysis was performed with Kaluza version 2.1 software. The panel used in this study is shown in Supplementary Table 1.

CCR5 receptor occupancy

We determined CCR5 receptor occupancy by leronlimab using phycoerythrin-labeled leronlimab (IncellDx Inc.) in a competitive flow cytometry assay. CCR5-expressing immune cells including

CD4+, CD45RO+ T-lymphocytes, CD4+, FoxP3+ T-regulatory cells, and CD14+, CD16+ monocytes/macrophages were included in the panel using the appropriate immunophenotypic markers for each population in addition to phycoerythrin-labeled leronlimab. Cells were incubated for 30 min in the dark at room temperature and washed twice with 2% BSA solution. Flow acquisition was conducted with a three-laser CytoFLEX fitted with 405 nm (80 mW), 488 nm (50 mW), and 638 nm (50 mW) lasers (Beckman Coulter, Indianapolis, IN, USA). Receptor occupancy was determined based on the loss of CCR5 detection over time in the subpopulations, and calculated using the following equation: $1 - A/B \times 100$, where A is day 0 and B is day 7.

Measurement of plasma SARS-CoV-2 viral loads

A QIAamp Viral Mini Kit (Qiagen, Catalog #52906) was used to extract nucleic acids from 300 to 400 μL of plasma sample according to the manufacturer's instructions and eluted in 50 μL of AVE buffer (RNase-free water with 0.04% sodium azide). The purified nucleic acids were tested immediately with a Bio-Rad SARS-CoV-2 ddPCR Kit (Bio-Rad, Hercules, CA, USA). The panel was designed for specifically detecting 2019-nCoV (two primer/probe sets). An additional primer/probe set was used to detect the human RNase P gene in control samples and clinical specimens. RNA isolated and purified from the plasma samples (5.5 μL) was added to a master mix comprising 1.1 μL of 2019-nCoV triplex assay, 2.2 μL of reverse transcriptase, 5.5 μL of supermix, 1.1 μL of dithiothreitol, and 6.6 μL of nuclease-free water.

The mixtures were then fractionated into up to 20,000 nanoliter-sized droplets in the form of a water-in-oil emulsion in a QX200 Automated Droplet Generator (Bio-Rad, Hercules, CA). The 96-well real-time-digital droplet polymerase chain reaction (RT-ddPCR) ready plate containing droplets was sealed with foil using a plate sealer and thermocycled to reverse transcribe the RNA, before PCR amplification of cDNA in a C1000 Touch thermocycler (Bio-Rad, Hercules, CA, USA). After PCR, the plate was loaded into a QX200 Droplet Reader (Bio-Rad, Hercules, CA, USA) and the fluorescence intensity of each droplet was measured in two channels (FAM and HEX). The fluorescence data were then analyzed with QuantaSoft 1.7 and QuantaSoft Analysis Pro 1.0 Software (Bio-Rad, Hercules, CA, USA) to determine the presence of SARS-CoV-2 N1 and N2 in the specimen. The limit of detection (LOD) was determined as shown in Supplementary Figure 1.

Bio-Rad SARS-CoV-2 RT-ddPCR Thermal Cycling Protocol

Cycling Step	Temperature (°C)	Time	Number of Cycles
Reverse Transcription	50	60 min	1
PCR Enzyme Activation	95	10 min	1
Template Denaturation	94	30 s	40
Annealing/Extension	55	60 s	
Droplet Stabilization	4	30 min	1
Hold (Optional)	4	Overnight	1

10. × Genomics 5′ single-cell RNA sequencing

Cells were then diluted to a concentration of 1 million cells per mL before loading onto the 10× chip. A single-cell RNA sequencing library was prepared with Chromium Next GEM Single cell Immune Profiling (v.1.1 Chemistry) according to the manufacturer's protocols using a Chromium Controller instrument. The library was sequenced using a High Output Flowcell and Illumina NextSeq 500 instrument. The healthy control reference data were obtained from public 10× genomics data sets ("5k_pbmc_v3" and "pbmc4k" from https://support.10xgenomics.com/single-cell-gene-expression/datasets, and "vdj_nextgem_hs_pbmc3" from https://support.10xgenomics.com/single-cell-vdj/datasets). Raw FASTQ reads for the experimental samples and reference data were processed using 10× Genomics Cellranger version 3.1.0, where the data were aligned with human genome build GRCh38. p13, including unplaced contigs. The Ensembl release 98 gene build was used for feature counting. The raw count matrix provided by Cellranger was filtered using EmptyDrops, and processed using Seurat version 3.1.4. Briefly, count matrices were imported for each sample, merged, and processed using a standard Seurat pipeline. Cells were filtered based on the following criteria: less than 200 or more than 3000 distinct genes, more than 15% unique molecular identifiers from mitochondrial genes, and a maximum library size of 20,000. Log normalization was then performed and the top variable genes were identified using the "vst" method. Differential expression (DE) analysis was performed using the Wilcoxon rank-based test based on the normalized counts. Only pertinent cells were used in the contrast for the cell-type DE level. In each comparison, the inclusion criteria for significant genes were set with the Bonferroni adjusted *p*-values generated with Seurat's FindMarkers function, with an error rate less than 0.1.

Statistical analysis

We performed statistical analyses between groups using the nonparametric Kruskal–Wallis test followed by Dunn's multiple comparison correction to control the experiment-wise error rate. We compared categorical variables using Fisher's exact test and continuous variables with the Mann–Whitney *U* test We assessed data based on the repeated measure correlation (rmcorr).

Results

Ten critical COVID-19 patients at the Montefiore Medical Center received leronlimab via FDA-approved EIND requests for individual patient use (Table 1). These confirmed SARS-CoV-2 positive patients had significant pre-existing co-morbidities and were receiving intensive care treatment, including mechanical ventilation or supplemental oxygen for ARDS. Consistent with previous reports of severe COVID-19 disease (Huang et al., 2020), these patients showed evidence of lymphopenia with liver and kidney damage (Supplementary Figure 2) (Akalin et al., 2020). Four of the patients died during the 14-day study period due to a combination of disease complications and severe constraints on medical equipment culminating in medical triage. Although this EIND study lacked a placebo control group for comparison, a recent study of other critically ill COVID-19 patients in the New York City area indicated mortality rates as high as 88% (Richardson et al., 2020).

Hyper-immune activation and CRS are present in cases of severe COVID-19 (Mehta et al., 2020). Indeed, at leronlimab treatment baseline, signatures of CRS were present in the plasma of all 10 patients in the form of significantly elevated levels of the inflammatory cytokines IL-1β, IL-6, and IL-8 (Figure 1A–C) compared with the healthy controls. In contrast to patients with mild or moderate COVID-19, only IL-6 was present at significantly higher levels in the critically ill patients. It should be noted that the plasma CCL5 levels of the 10 critically ill patients were markedly elevated compared with those of both the healthy controls and mild or moderate COVID-19 patients (Figure 1D). High levels of CCL5 can cause acute renal failure and liver toxicity (Yu et al., 2016; Chen et al., 2020), which are both common findings with COVID-19 infection. Indeed, the critically ill patients presented with varying

Table 1
Leronlimab-treated critical COVID-19 patient summaries.

Patient	Age/ Gender	Pre-existing conditions	Renal transplant year	Dialysis in hospital	Day relative to leronlimab			Treatments for COVID and concomitant infections	Vasopressors used	Baseline status	Extubated (day relative to leronlimab)	Respiratory outcome	Subject status (day relative to leronlimab)
					Onset Sx	PCR +	Admit						
L1	74/M	AKI, HTHD, Prostate CA (s/p prostatectomy), DM, Gout	N/A	Yes	−14	−8	−8	CQ, HCQ, TZP, AZT	Yes	Intubated	TBD	Remains intubated	Still admitted
L2	74/F	ESRD, HTHD, DM, HLD	2018	Yes	−3	−2	−2	HCQ, CQ, AZM, LPV/RTV	Yes	Intubated	No	Worsened	Deceased (8)
L3	54/M	RF, HTHD, HLD	N/A	Yes	−1	−1	−1	CQ, HCQ, TZP, VAN	Yes	Venture mask, same day intubated	TBD	Remains intubated	Still admitted
L4	56/M	HTHD, Skin CA, Papillary thyroid CA (s/p thyroidectomy), DM	N/A	Yes	−1	2	−8	CQ, LPV/RTV	Yes	Intubated	Yes (1)	RA by day 8	Still admitted
L5	58/M	ESRD, CKD stage 3 in renal allograft, recurrent UTI with MDR E.coli, DM, DR, HTHD, HLD	2016	Yes	−8	−5	−6	AZM, HCQ	Yes	Intubated	Yes (13)	Improving	Still admitted
L6	42/M	FSGS, CKD stage 3, DVT/PE, Gout	2005, 2016	No	−4	−1	−1	HCQ, AZM, CAX, VAN, CEF	No	On 2 L NC	N/A	Stable on RA	Discharged (13)
L7	68/M	ESRD, Hydronephrosis (s/p stent placement), HTHD, HLD, DM with retinopathy and neuropathy	2018	Yes	−13	−10	−10	AZM, HCQ, VAN, TZP	Yes	On NRB	TBD	Improving	Still admitted
L8	56/F	ESRD, lung CA (s/p bilateral upper lobectomy), COPD, Asthma, DM, HTHD, HLD, Hepatitis C	2009	No	−7	−5	−5	CAX, AZT, HCQ, CEF, VAN	No	3−4 L NC[a]	No	Worsened	Deceased (6)
L9	51/F	AKI, HTHD, OSA (on Bilevel Positive Airway Pressure)	2006	Yes	−6	−5	−6	HCQ	Yes	Intubated	No	Worsened	Deceased (4)
L10	79/M	AKI, CAD, Prostate CA, GERD, HTHD, HLD	N/A	Yes	−13	−6	−6	HCQ	Yes	Intubated	No	Remained intubated	Deceased (7)

N/A = not applicable, s/p = status post-, AKI = acute kidney injury, HTHD = hypertensive heart disease, DM = diabetes mellitus, HLD = hyperlipidemia, ESRD = end-stage renal disease, HD = hemodialysis, CA = cancer, COPD = chronic obstructive pulmonary disease, LUL = left upper lobe, RUL = right upper lobe, MDR = multi-drug resistant, CKD = chronic kidney disease, UTI = urinary tract infection, FSGS = focal segmental glomerulosclerosis, DVT = deep vein thrombosis, PE = pulmonary embolism, OSA = obstructive sleep apnea, CAD = coronary artery disease, GERD = gastroesophageal reflux disease, RF = renal failure, DR = diabetic retinopathy, HCQ = hydroxychloroquine, CQ = chloroquine, AZM = azithromycin, VAN = vancomycin, CAX = ceftriaxone, LPV/RTV = lopinavir/ritonavir, TZP = piperacillin-tazobactam, CEF = cefepime, NC = nasal canula, NRB = non-rebreather mask, TBD = to be determined.

[a] Patient declined intubation due to poor baseline pulmonary status.
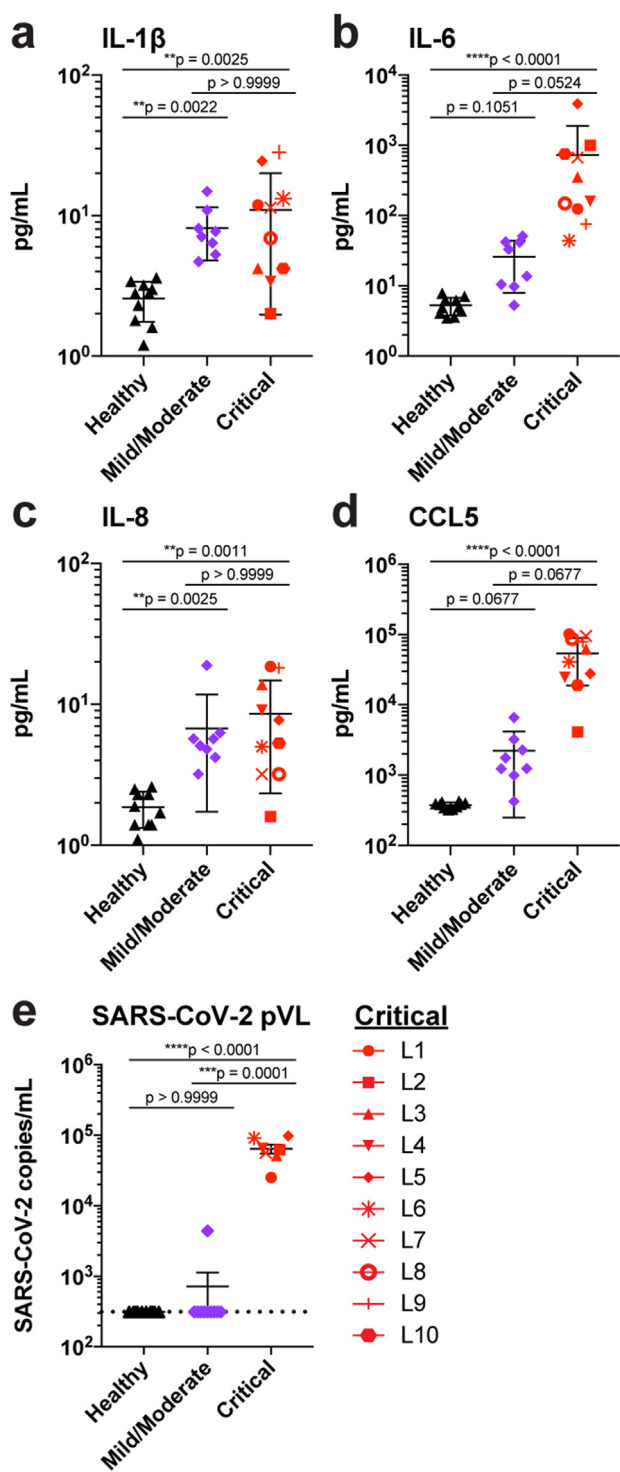
Figure 1. Elevated cytokine, chemokine, and SARS-CoV-2 levels in critically ill COVID-19 patients. (A–E) Plasma levels of IL-1β (A), IL-6 (B), IL-8 (C), CCL5 (D), and SARS-CoV-2 RNA copies (E) in patients with mild/moderate (purple symbols, n = 8) and critical (red symbols, n = 10 in panels a–d, and n = 7 in panel e) COVID-19 disease compared with healthy controls (black symbols, n = 10). Dashed line indicates the LOD. Graphs show *p*-values calculated using Dunn's Kruskal–Wallis test: *$p \leq 0.05$, ** $p \leq 0.01$, ***$p \leq 0.001$, ****$p \leq 0.0001$.

degrees of kidney and liver injury, although many had also previously received kidney transplants (Akalin et al., 2020) (Table 1 and Supplementary Figure 2). Low levels of SARS-CoV-2 have been detected but not yet quantified in the plasma of COVID-19 patients (Lescure et al., 2020). We used high sensitivity, ddPCR to quantify

plasma SARS-CoV-2 viremia at baseline. SARS-CoV-2 was found in the plasma of all 10 critically ill patients, but no viremia was detected in the healthy controls and in only one patient with mild/moderate COVID-19, thereby highlighting the critical nature of COVID-19 in these patients (Figure 1E).

At study day 0, all 10 critically ill patients received a subcutaneous injection of 700 mg leronlimab following baseline blood collection. Subsequently, the patients received a second subcutaneous injection of 700 mg leronlimab at study day 7. The defining features of severe COVID-19 disease include the plasma IL-6 and T cell lymphopenia (Huang et al., 2020; Lescure et al., 2020), so we longitudinally monitored these parameters for 2 weeks after the first leronlimab treatment. A reduction in the plasma IL-6 was observed as early as 3 days following leronlimab with a return to healthy control levels by day 14 (Figure 2A). In contrast to IL-6, the levels of other cytokines and chemokines were more variable after leronlimab treatment (Supplementary Figure 3). Following leronlimab administration, a marked restoration of CD8+ T cells (Figure 2B) and normalization of the CD4+ and CD8+ T cell ratio were observed in the blood samples (Figure 2C). These immunological changes occurred concomitant with leronlimab CCR5 receptor occupancy on the surface of CCR5+ T cells and monocytes (Figure 2D and E). The percentage of other CCR5-expressing cell types (CD4 T-cells, NK cells, and monocyte/macrophages) did not change significantly over 14 days of leronlimab treatment. Following leronlimab administration, SARS-CoV-2 plasma viremia decreased in all patients at day 7, and all but one patient had resolved SARS-CoV-2 plasma viremia to undetectable levels by day 14 (Figure 2F left, *p* = 0.0012). Finally, SARS-CoV-2 plasma viremia in leronlimab-treated COVID-19 patients was inversely correlated with the frequency of CD8+ T cells in the blood, which suggested immune restoration (Figure 2G).

To establish an unbiased gene repertoire for these COVID-19 patients, we performed 10× Genomics 5′ single cell RNA sequencing for PBMCs from two of the severe COVID-19 patients (L2 and L4) for which sufficient baseline, pre-leronlimab treatment COVID-19 samples were available. We also performed scRNA-seq for the same patients at day 7 post-treatment, and included three reference PBMC scRNA-seq data sets from healthy controls provided by 10× Genomics. After quality control, our longitudinal COVID-19 single cell data set profiled a total of 3785 cells at baseline, 5056 cells at the 7-day post-leronlimab time point, and 18,603 cells from healthy controls. We were able to assign cell types to most cells based on a combination of the expression of known marker genes and automated cell type classification using the SingleR package (Aran et al., 2019) to identify five primary clusters that corresponded to monocytes, B, T, and NK cells, and some platelets (Figure 3). We initially compared the baseline COVID samples with the healthy controls. We detected a total of 75 DE transcripts (Wilcoxon adjusted *p* < 0.1) (Supplementary Table 2). The top pathways enriched in this set included multiple TCR signaling pathways, such as the genes LCK, CD3E, and NFKBIA (Figure 3). Differences in cellularity between donors will confound global gene expression analyses, so we extracted the myeloid cell cluster and performed DE analyses using only these cells. We identified 131 DE transcripts between the healthy controls and COVID-19 on day 0 (Supplementary Table 2 and Figure 3). This gene set was enriched for genes involved in interferon signaling (IFITM2, IFNGR2, and NFKBIA), and cytokine signaling (HSP8A, JUN, and TIMP1). We found that several downstream targets of IL-6 were also upregulated: ZFP36L2, CEBPB, and LY6E.

To identify markers that could inform effective leronlimab treatment, we then compared gene expression within the two severe COVID-19 participants by contrasting the baseline and day 7 post-leronlimab. After performing bulk DE based on the total
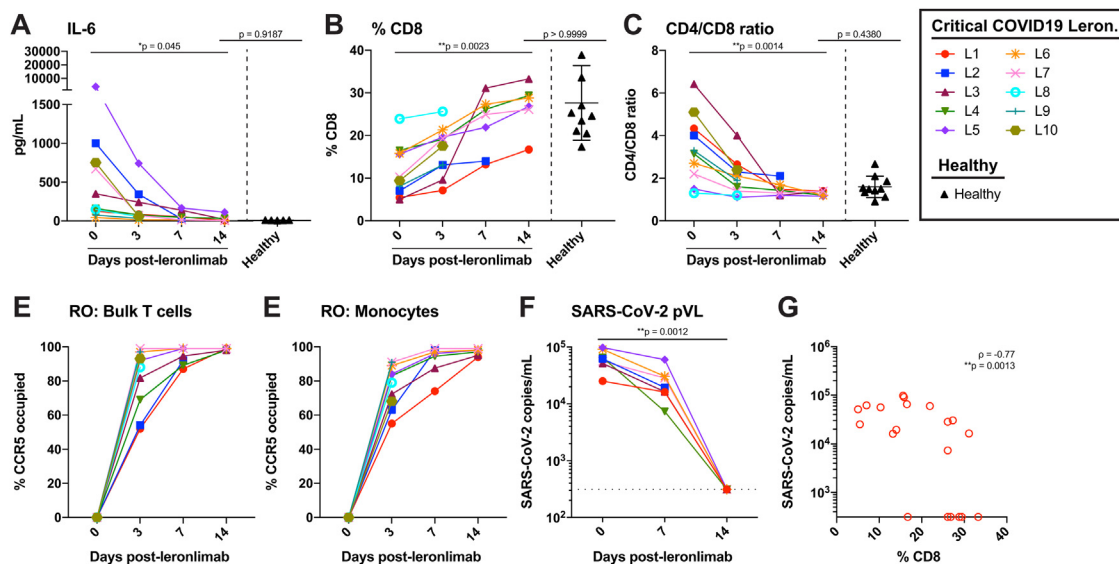
Figure 2. Reversal of immune dysfunction, CCR5 receptor occupancy, and decrease in SARS-CoV-2 plasma viral loads in critically ill COVID-19 patients after leronlimab administration. (A–C) Plasma levels of IL-6 (A), and peripheral blood CD8+ T cell percentages of CD3+ cells (B) and CD4/CD8 T cell ratio (C) at days 0 (n = 10), 3 (n = 10), 7 (n = 7), and 14 (n = 6) post-leronlimab administration. Healthy controls (n = 10) are shown in black triangles. Critically ill COVID-19 patients not treated with leronlimab are shown in panel A (right, open symbols, n = 5). Graphs show p-values calculated using Dunn's Kruskal–Wallis test: not significant $p > 0.05$, *$p \leq 0.05$, ** $p \leq 0.01$, ***$p \leq 0.001$, ****$p \leq 0.0001$. (D–E) CCR5 receptor occupancy on peripheral blood bulk T cells (D), and monocytes (E). (F), SARS-CoV-2 plasma viral loads at days 0, 7, and 14 post-leronlimab (left panel, closed symbols, n = 7). Critically ill COVID-19 patients not treated with leronlimab are shown in panel F (right panel, open symbols, n = 5). Horizontal dashed line indicates the LOD. Graph show p-values calculated using the Mann–Whitney test: *$p \leq 0.05$, ** $p \leq 0.01$, ***$p \leq 0.001$, ****$p \leq 0.0001$. (G) Plot showing CD8 percentages in blood and SARS-CoV-2 plasma viral load in seven critically ill COVID-19 patients at days 0, 7, and 14 post-leronlimab (n = 20). Graph shows rho (ρ) and p- values calculated by repeated measures correlation: *$p \leq 0.05$, ** $p \leq 0.01$, ***$p \leq 0.001$, ****$p \leq 0.0001$. The 95% confidence interval for the repeated measures correlation was −0.93 to 0.35.

PBMCs, we identified 14 DE genes, although this could also have been confounded by the differences in the cell compositions. It should be noted that this set included a significant drop in CD44, a downstream target of IL-6 signaling (Vincent and Mechti, 2004), and a number of genes involved in neutrophil degranulation (ITGB2, EEF2, HSP90AA1, and ALDOA). Next, we performed DE specifically based on myeloid cells and identified 73 DE transcripts in this subset (Wilcoxon adjusted $p < 0.1$; Supplementary Table 2). In agreement with the decrease in the IL-6 protein levels observed in plasma, we observed significant decreases in the expression of many IL-6 responsive genes, including TGFB1, IFI30, and LY6E, which are consistent with previous reports of monocyte/macrophages repolarization following CCR5 blockade (Halama et al., 2016). We also observed myeloid cells expressing chemokine and IFN-related genes, such as IFNGR2, IFITM2, and TALDO1, which were significantly downregulated at day 7 post-leronlimab compared with baseline (Supplementary Table 2). These transcriptomic findings further highlight the potential impact of leronlimab-mediated CCR5 blockade on the inflammatory state in COVID-19.

Discussion

In this study, we investigated the involvement of the chemokine receptor CCR5 in COVID-19 and obtained data from 10 critically ill patients with severe COVID-19 that demonstrated reductions in inflammation, restoration of T cell lymphocytopenia, and reduced SARS-CoV-2 plasma viremia following leronlimab-mediated CCR5 blockade. We found statistically significant increases in IL-1β, IL-6, IL-8, and RANTES in these critically ill patients compared with healthy controls. The increases in these cytokines are the hallmark of COVID-19 and elevation of the chemokine CCL5/RANTES has been demonstrated across the COVID-19 disease spectrum from mild (Zhao et al., 2020) to severe (Li et al., 2020) patients. RANTES

was elevated to a greater extent than the other CCR5 binding chemokines MIP-1α and MIP-1β, probably due to the production of RANTES in respiratory epithelial cells (in addition to immune cells) in respiratory viral infections (Schroth et al., 1999). We also found a profound reduction in the CD8 percentage with concomitant increases in the CD4/CD8 ratio. In this cohort of critical COVID-19 patients, SARS-CoV-2 RNA was detectable and quantifiable in plasma samples from all patients. For the first time, we demonstrated that restoration of the CD8 T-cell numbers was significantly correlated with decreases in the plasma viral load. Overall, our results showed that therapy with a CCR5 antagonist could reduce the cytokine storm, resolve the profound CD-8 T-cell lymphopenia, and reduce the plasma viral load to undetectable levels by day 14. These data support recent studies that suggested the potential for targeting CCR5 as a therapeutic in COVID-19 (Chua et al., 2020).

Recent studies showed that a significant number of COVID-19 patients had increased risks of strokes, blood clots, and other thromboembolic events (Grillet et al., 2020). Platelet activation leads to initiation of the coagulation cascade and it can be triggered by chemokines including CCL5/RANTES (Machlus et al., 2016), thereby suggesting that leronlimab treatment may be beneficial beyond its immunomodulatory effects on inflammation and hemostasis in COVID-19 patients. Given medical triage resulting in patient death and the lack of a placebo control group, we cannot comment on the impact of leronlimab on the clinical outcomes in these patients. Anecdotal evidence has been reported of clinical improvements in COVID-19 patients following leronlimab treatment (Mottet, 2020), but randomized controlled trials are required to determine the efficacy of leronlimab in COVID-19. Indeed, randomized, double blind, placebo controlled clinical trials are underway to assess the efficacy of leronlimab treatments in patients with mild to
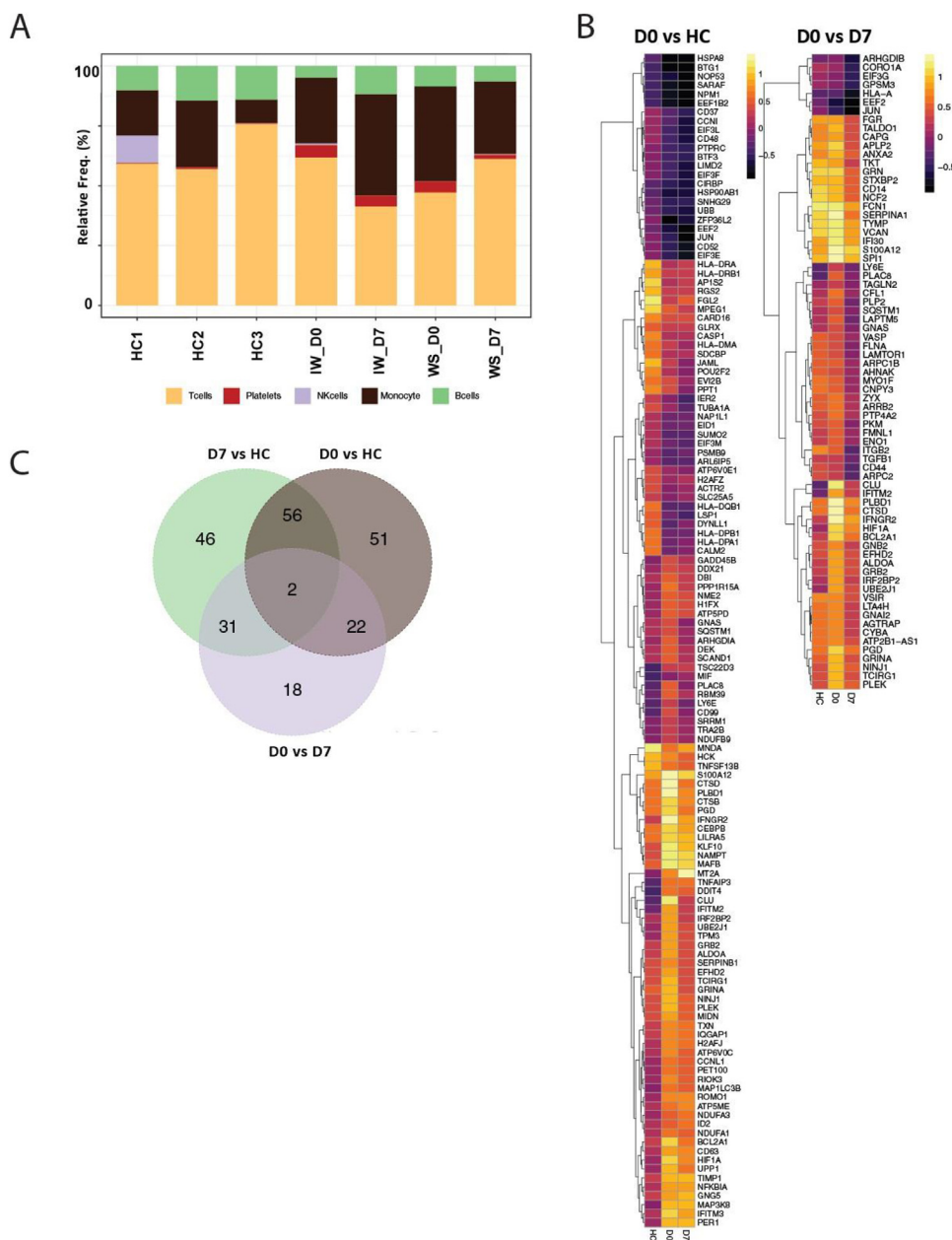
Figure 3. Phenotyping and differential gene expression analyses based on scRNA-seq data. (A) Graph showing the proportion of each cell type in healthy control and leronlimab-treated COVID patient samples. (B) Heatmap of significantly differentially expressed genes (Wilcoxon adjusted *p* < 0.1) by contrasting either COVID day 0 vs. healthy control (HC) or COVID day 9 vs day 7 post-leronlimab treatment. (C) Venn diagram showing the overlap between genes identified from the contrasts shown.

moderate (NCT04343651) (ClinicalTrials.gov, 2020) and severe to critical (NCT04347239) COVID-19 (ClinicalTrials.gov). In summary, our results suggest the involvement of CCR5 in the pathology of SARS-CoV-2, and that inhibiting the activity of CCL5 via CCR5/RANTES blockade represents a novel therapeutic strategy for COVID-19 with both immunological and virological implications.

Conflict of interest

Ethical approval

Approved.

Acknowledgments

Appendix A. Supplementary data

Supplementary material related to this article can be found, in the online version, at doi:https://doi.org/10.1016/j.ijid.2020.10.101.

References

Akalin E, Azzi Y, Bartash R, Seethamraju H, Parides M, Hemmige V, et al. Covid-19 and kidney transplantation. N Engl J Med 2020;, doi:http://dx.doi.org/10.1056/NEJMc2011117.

Aran D, Looney AP, Liu L, Wu E, Fong V, Hsu A, et al. Reference-based analysis of lung single-cell sequencing reveals a transitional profibrotic macrophage. Nat Immunol 2019;20:163–72.

Channappanavar R, Perlman S. Pathogenic human coronavirus infections: causes and consequences of cytokine storm and immunopathology. Semin Immunopathol 2017;39:529–39.

Chen L, Zhang Q, Yu C, Wang F, Kong X. Functional roles of CCL5/RANTES in liver disease. Liver Res 2020;4:28–34.

Chua RL, Lukassen S, Trump S, Hennig BP, Wendisch D, Pott F, et al. COVID-19 severity correlates with airway epithelium-immune cell interactions identified by single-cell analysis. Nat Biotechnol 2020;8:970–9.

ClinicalTrials.gov-Study to Evaluate the Efficacy and Safety of Leronlimab for Mild to ModerateCOVID-19. https://clinicaltrials.gov/ct2/show/NCT04343651.ClinicalTrials.gov, Study to Evaluate the Efficacy and Safety of Leronlimab for Patients with Severe or Critical Coronavirus Disease 2019 (COVID-19). https://clinicaltrials.gov/ct2/show/NCT04347239.

Dhody K, Pourhassan N, Kazempour K, Green D, Badri S, Mekonnen H, et al. PRO 140, a monoclonal antibody targeting CCR5, as a long-acting, single-agent maintenance therapy for HIV-1 infection. HIV Clin Trials 2018;19:85–93.

Grillet F, Behr J, Calame P, Aubry S, Delabrousse E. Acute pulmonary embolism associated with COVID-19 pneumonia detected by pulmonary CT angiography. Radiology 2020;, doi:http://dx.doi.org/10.1148/radiol.2020201544.

Halama N, Zoernig I, Berthel A, Kahlert C, Klupp F, Suarez-Carmona M, et al. Tumoral immune cell exploitation in colorectal cancer metastases can be targeted effectively by anti-CCR5 therapy in cancer patients. Cancer Cell 2016;29:587–601.

Huang C, Wang Y, Li X, Ren L, Zhao J, Hu Y, et al. Clinical features of patients infected with 2019 novel coronavirus in Wuhan, China. Lancet 2020;395:497–506.

Jacobson JM, Saag MS, Thompson MA, Fischl MA, Liporace R, Reichman RC, et al. Antiviral activity of single-dose PRO 140, a CCR5 monoclonal antibody, in HIV-infected adults. J Infect Dis 2008;198:1345–52.

Jacobson JM, Thompson MA, Lalezari JP, Saag MS, Zingman BS, D'Ambrosio P, et al. Anti-HIV-1 activity of weekly or biweekly treatment with subcutaneous PRO 140, a CCR5 monoclonal antibody. J Infect Dis 2010a;201:1481–7.

Jacobson JM, Lalezari JP, Thompson MA, Fichtenbaum CJ, Saag MS, Zingman BS, et al. Phase 2a study of the CCR5 monoclonal antibody PRO 140 administered intravenously to HIV-infected adults. Antimicrob Agents Chemother 2010b;54:4137–42.

Law HK, Cheung CY, Ng HY, Sia SF, Chan YO, Luk W, et al. Chemokine up-regulation in SARS-coronavirus-infected, monocyte-derived human dendritic cells. Blood 2005;106:2366–74.

Lescure FX, Bouadma L, Nguyen D, Parisey M, Wicky PH, Behillil S, et al. Clinical and virological data of the first cases of COVID-19 in Europe: a case series. Lancet Infect Dis 2020;, doi:http://dx.doi.org/10.1016/S1473-471.3099(20)30200-0.

Li S, Jiang L, Li X, Lin F, Wang Y, Li B, et al. Clinical and pathological investigation of patients with severe COVID-19. JCI Insight 2020;5(12)e138070, doi:http://dx.doi.org/10.1172/jci.insight.138070 PMID: 32427582.

Machlus KR, Johnson KE, Kulenthirarajan R, Forward JA, Tippy MD, Soussou TS, et al. CCL5 derived from platelets increases megakaryocyte proplatelet formation. Blood 2016;127:921–6.

Mehta P, McAuley DF, Brown M, Sanchez E, Tattersall RS, Manson JJ, et al. COVID-19: consider cytokine storm syndromes and immunosuppression. Lancet 2020;395:1033–4.

Mottet S. Coronavirus Survivor Credits Artificial Antibody Experimental Treatment for Recovery. Los Angeles CBS Local; 2020. https://losangeles.cbslocal.com/2020/04/10/coronavirus-survivor-leronlimab/.

Nicholls JM, Poon LL, Lee KC, Ng WF, Lai ST, Leung CY, et al. Lung pathology of fatal severe acute respiratory syndrome. Lancet 2003;361:1773–8.

Olson WC, Rabut GE, Nagashima KA, Tran DN, Anselma DJ, Monard SP, et al. Differential inhibition of human immunodeficiency virus type 1 fusion, gp120 binding, and CC-chemokine activity by monoclonal antibodies to CCR5. J Virol 1999;73:4145–55.

Qin C, Zhou L, Hu Z, Zhang S, Yang S, Tao Y, et al. Dysregulation of immune response in patients with COVID-19 in Wuhan, China. Clin Infect Dis 2020;71:762–8.

Richardson S, Hirsch JS, Narasimhan M, Crawford JM, McGinn T, Davidson KW, et al. Presenting characteristics, comorbidities, and outcomes among 5700 patients hospitalized with COVID-19 in the New York City Area. JAMA 2020;26(323):2052–9.

Schroth MK, Grimm E, Frindt P, Galagan DM, Konno S-I, Love R, et al. Rhinovirus replication causes RANTES production in primary bronchial epithelial cells. Am J Respir Cell Mol Biol 1999;20:1220–8.

Vincent T, Mechti N. IL-6 regulates CD44 cell surface expression on human myeloma cells. Leukemia 2004;18:967–75.

World Health Organization. Coronavirus Disease (COVID-2019) Situation Reports. Available at: https://www.who.int/emergencies/diseases/novel-coronavirus-2019/situation-reports. [Accessed 23 April 2020].

Yen YT, Liao F, Hsiao CH, Kao CL, Chen YC, Wu-Hsieh BA. Modeling the early events of severe acute respiratory syndrome coronavirus infection in vitro. J Virol 2006;80:2684–93.

Yu TM, Palanisamy K, Sun KT, Day YJ, Shu KH, Wang IK, et al. RANTES mediates kidney ischemia reperfusion injury through a possible role of HIF-1α and LncRNA PRINS. Sci Rep 2016;6:18424.

Zhao Y, Qin L, Zhang P, Li K, Liang L, Sun J, et al. Longitudinal COVID-19 profiling associates IL-1RA and IL-10 with disease severity and RANTES with mild disease. JCI Insight 2020;5:e139834.